

**Singly ionizing 100-MeV/amu C<sup>6+</sup> + He collisions with small momentum transfer**

Konstantin A. Kouzakov\*

*Department of Nuclear Physics and Quantum Theory of Collisions, Faculty of Physics, Lomonosov Moscow State University, Moscow 119991, Russia and Skobel'syn Institute of Nuclear Physics, Lomonosov Moscow State University, Moscow 119991, Russia*

Sergey A. Zaytsev

*Department of Physics, Khabarovsk State Technical University, Tikhoookanskaya 136, Khabarovsk 680035, Russia*

Yuri V. Popov

*Skobel'syn Institute of Nuclear Physics, Lomonosov Moscow State University, Moscow 119991, Russia*

Masahiko Takahashi

*Institute of Multidisciplinary Research for Advanced Materials, Tohoku University, Sendai 980-8577, Japan*

(Received 12 August 2012; published 25 September 2012)

We present a theoretical analysis of single ionization of He by C<sup>6+</sup> at an impact energy of 100 MeV/amu and a momentum transfer  $Q = 0.75$  a.u. Relativistic, second-order Born, and distorted-wave effects on fully differential cross sections are examined. It is demonstrated that neither of them is able to explain the serious discrepancy observed between theory and experiment when an electron is ejected perpendicular to the direction of momentum transfer. We show, however, that experimental uncertainties, including those due to a velocity spread of the He gas atoms in a supersonic jet, can be responsible for the observed disagreement.

DOI: [10.1103/PhysRevA.86.032710](https://doi.org/10.1103/PhysRevA.86.032710)

PACS number(s): 34.50.Fa, 52.20.Hv

**I. INTRODUCTION**

Ionization processes in collisions of charged projectiles with atomic systems are of fundamental importance for the physics of interaction of particles and radiations with matter. The basic theory of such processes in the case of fast ionic projectiles is well established (see, for instance, the textbooks [1–3]). In particular, it is expected that at  $|Z_p|/v_p \ll 1$ , where  $Z_p$  and  $v_p$  are the projectile charge and velocity, respectively, perturbation theory should be well applicable. The emergence of the cold-target-recoil-ion-momentum spectroscopy (COLTRIMS) [4,5] made it possible to measure fully differential cross sections for the ionizing ion-atom collisions with high precision, thus providing a very stringent test of the theory. In this context, theoretical interpretation of the experimental results on singly ionizing 100-MeV/amu C<sup>6+</sup>+He collisions ( $Z_p/v_p \sim 0.1$ ), which were reported by Schulz *et al.* [6] almost a decade ago, cannot be regarded as satisfactory. So far none of the published theoretical investigations, ranging from first Born approximation [6,7] and second Born approximation [8,9] to continuum or three-body distorted-wave [10,11] and coupled-pseudostate models [9,12], has been able to obtain reasonable agreement with the measured angular distribution of the ejected electron in the plane perpendicular to the momentum transfer  $\mathbf{Q}$ . The marked discrepancies between theory and experiment are determined in that plane, both in shape and in magnitude. Namely, the theory strongly underestimates the experimental intensity and yields almost flat angular distribution for the ejected electron, while the experiment exhibits two well-pronounced peaks. At the same time, all the approaches more or less adequately

reproduce the measured angular distribution of the ejected electron in the scattering plane.

In Ref. [13] the discrepancies were attributed to experimental uncertainties of the measurements [6], which are due to a finite energy and angle resolution as well as to a velocity spread of the He gas atoms in a supersonic jet caused by its nonzero temperature. However, this explanation was later refuted in Ref. [14], where the experimental data of Ref. [6] were analyzed with a Monte Carlo event generator based on quantum theory. The role of the experimental uncertainties was found to be important in the subsequent papers [15–17], where they were taken into account in the calculations based on a theoretical model in which the C<sup>6+</sup> projectile first ionizes the electron and then scatters elastically off the recoil ion. Though such a treatment explains much of the observed differences, the validity of the employed elastic scattering model is questionable, for it treats the two collisions (inelastic and elastic) incoherently. The latter approach apparently lacks grounds from a quantum mechanical viewpoint. Recently Colgan *et al.* [18] have examined the problem using the time-dependent close-coupling method within the impact-parameter theory [19]. They introduced in their calculations the phase factor that accounts for the internuclear interaction. In this way they obtained two peaks, whose positions agree with those seen in the experiment. However, the theory still substantially underestimates the experiment. In a very recent study [20], using a nonperturbative impact-parameter coupled-pseudostate approximation, dips instead of peaks have been found, thus not supporting the results of Ref. [18].

In the present work we revisit the C<sup>6+</sup> problem. Our theoretical analysis examines various basic approaches. These include the relativistic and nonrelativistic first-order perturbation theories, second Born approximation, and distorted-wave Born approximation. It is shown by numerical calculations that they are unable to explain the disagreement between theory

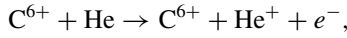
\*kouzakov@srd.sinp.msu.ru

and experiment, all yielding more or less similar results. We also inspect the roles of the momentum uncertainties in the experiment under consideration. It is demonstrated that they can be crucial in resolving the “C<sup>6+</sup> puzzle.” A distinct feature of our analysis is that all calculations are performed using the same initial- and final-state wave functions of the He atom. This allows us to examine the discussed theoretical approaches and effects on equal footing.

The paper is organized as follows. In Sec. II, we formulate different theoretical models and approximations for the considered process. Then, in Sec. III, we compare numerical results to experiment. The conclusions are drawn in Sec. IV. Atomic units (a.u.) in which  $\hbar = e = m_e = 1$  are used throughout unless otherwise stated.

## II. THEORY

In our analysis we consider the following single-ionization reaction:



which is induced by impact of a relativistic fully stripped carbon ion at small energy and momentum transfer values. We specify the initial and final four-momenta of C<sup>6+</sup> by  $k = (E_p/c, \mathbf{k}_p)$  and  $k' = (E'_p/c, \mathbf{k}'_p)$ , respectively, the energy-momentum transfer by  $q = (T/c, \mathbf{Q})$ , where  $T = E_p - E'_p$  and  $\mathbf{Q} = \mathbf{k}_p - \mathbf{k}'_p$ , and the kinetic energy and momentum of the ejected electron by  $E_e$  and  $\mathbf{k}_e$ , respectively. The He atom is assumed to be initially in the ground state and at rest in the laboratory frame. Note that under the discussed kinematical conditions the velocity of the recoil He<sup>+</sup> ion in that frame is negligibly small. We will consider an impact energy of 100 Mev/amu and the case of  $E_e = 6.5$  eV and  $Q = 0.75$  a.u. [6], which is the most significant example of discrepancies between theory and experiment for the discussed process (other cases can be found, for instance, in Madison *et al.* [7]).

We focus on the fully differential cross section (FDCS), which is differential in the projectile solid angle  $\Omega_p$ , electron solid angle  $\Omega_e$  and kinetic energy  $E_e$ . In the laboratory frame it can be presented as follows [2]:

$$\frac{d^3\sigma}{dE_e d\Omega_e d\Omega_p} = \frac{k_e E_p'^2 k'_p}{(2\pi)^5 c^4 k_p} |\mathcal{T}_{fi}|^2, \quad (1)$$

where the normalization volume is set to unity, and  $\mathcal{T}_{fi}$  is the scattering amplitude. One should be careful when performing the nonrelativistic limit of Eq. (1). The latter limit implies, in particular, that  $E_p/c^2 = E'_p/c^2 = M_p$ , where  $M_p$  is the rest mass of C<sup>6+</sup>. However, this is a rather crude approximation in the case of the discussed impact energy value (100 Mev/amu), which gives the projectile's Lorentz factor of about 1.1. Therefore, in what follows we use relativistic kinematical variables of the projectile, even when employing the nonrelativistic approximations for the scattering amplitude (see below).

### A. First-order perturbation theory

Collisions of fast charged particles with atomic systems are usually treated to lowest order in the projectile-target interac-

tion. In quantum electrodynamics (QED) the corresponding scattering amplitude is given by [2]

$$\mathcal{T}_{fi}^{\text{QED}} = \frac{1}{c^2} D_{\mu\nu}(q^2) J_{fi}^\mu(-q) J_{kk'}^\nu(q), \quad (2)$$

where  $D_{\mu\nu}$  is the photon propagator and  $J_{fi}$  and  $J_{kk'}$  are the electromagnetic transition four-currents of He and C<sup>6+</sup>, respectively.

The amplitude (2) is gauge invariant. We choose the photon propagator in the Feynman gauge,

$$D_{\mu\nu}(q^2) = \frac{4\pi c^2 g_{\mu\nu}}{T^2 - Q^2 c^2}, \quad (3)$$

where  $g_{\mu\nu}$  is the metric tensor. The He transition four-current can be treated nonrelativistically, so that

$$J_{fi}(-q) = (c\rho_{fi}(\mathbf{Q}), \mathbf{j}_{fi}(\mathbf{Q})), \quad (4)$$

with [2]

$$\begin{aligned} \rho_{fi}(\mathbf{Q}) &= \langle \Psi_f | \sum_{j=1}^2 e^{i\mathbf{Q}\cdot\mathbf{r}_j} | \Psi_i \rangle, \\ \mathbf{j}_{fi}(\mathbf{Q}) &= -\frac{i}{2} \langle \Psi_f | \sum_{j=1}^2 (e^{i\mathbf{Q}\cdot\mathbf{r}_j} \nabla_j + \nabla_j e^{i\mathbf{Q}\cdot\mathbf{r}_j}) | \Psi_i \rangle, \end{aligned}$$

where  $\Psi_{i(f)}$  is the ground-state (final-state) wave function of He. Since C<sup>6+</sup> is a scalar particle, its transition four-current is [2]

$$J_{kk'}(q) = \frac{(k+k')c^2}{2\sqrt{E_p E'_p}} f(q^2), \quad (5)$$

where  $f(q^2)$  is the electromagnetic form factor of C<sup>6+</sup>, which in the discussed case here of small  $T$  and  $Q$  values reduces to  $f(q^2) = Z_p$  ( $Z_p = 6$ ).

Substituting Eqs. (3)–(5) in Eq. (2) and taking into account that

$$T\rho_{fi}(\mathbf{Q}) - \mathbf{Q} \cdot \mathbf{j}_{fi}(\mathbf{Q}) = 0,$$

we get

$$\mathcal{T}_{fi}^{\text{QED}} = \frac{1}{1 - \frac{T^2}{Q^2 c^2}} \sqrt{\frac{E_p}{E'_p}} \left[ 1 - \frac{\mathbf{v}_p \cdot \mathbf{j}_{fi}(\mathbf{Q})}{c^2 \rho_{fi}(\mathbf{Q})} \right] \mathcal{T}_{fi}^{\text{FBA}}, \quad (6)$$

where  $\mathbf{v}_p = \mathbf{k}_p c^2 / E_p$  is the incident velocity of C<sup>6+</sup> and

$$\mathcal{T}_{fi}^{\text{FBA}} = -\frac{4\pi Z_p}{Q^2} \rho_{fi}(\mathbf{Q}) \quad (7)$$

is the nonrelativistic lowest-order scattering amplitude [1] that amounts to the first Born approximation (FBA).

### B. Second Born approximation

Effects beyond the FBA are typically estimated within the second Born approximation (SBA). For the present case it takes the form,

$$\mathcal{T}_{fi}^{\text{SBA}} = \mathcal{T}_{fi}^{\text{FBA}} + \delta\mathcal{T}_{fi}^{\text{SBA}}, \quad (8)$$

where the SBA contribution evaluates as

$$\delta\mathcal{T}_{fi}^{\text{SBA}} = \sum_n \int \frac{d^3p}{(2\pi)^3} \frac{4\pi Z_p}{(\mathbf{Q}-\mathbf{p})^2} \frac{4\pi Z_p}{p^2} \times \frac{[\rho_{fn}(\mathbf{Q}-\mathbf{p}) - 2\delta_{fn}][\rho_{ni}(\mathbf{p}) - 2\delta_{ni}]}{\mathbf{v}_p \cdot \mathbf{p} + \varepsilon_i - \varepsilon_n + i0}. \quad (9)$$

Here the  $n$  sum runs over all helium states, with  $\varepsilon_n$  being their energies, and the terms  $\sim v_p p^2/k_p$  are neglected in the denominator of the Green's function in the integrand.

Direct calculation of (9) is not possible, for its value diverges (specifically, when  $n = f$ ), reflecting the fact that the plane waves are not correct asymptotic states of the projectile in the problem of Coulomb breakup (see Ref. [21] and references therein). However, even after being properly renormalized [21], it is still not tractable numerically with the present computational facilities. One of the most commonly utilized approaches to evaluate the SBA term is the closure approximation, where the intermediate target excitation energies are set to an average value,

$$\varepsilon_n - \varepsilon_i = \bar{\varepsilon}, \quad (10)$$

called the closure parameter.

In the closure approximation (10) the SBA term (9) acquires the form,

$$\delta\mathcal{T}_{fi}^{\text{SBA}} = \int \frac{d^3p}{(2\pi)^3} \frac{4\pi Z_p}{(\mathbf{Q}-\mathbf{p})^2} \frac{4\pi Z_p}{p^2} \times \frac{\rho_{fi}(\mathbf{Q}) - 2\rho_{fi}(\mathbf{Q}-\mathbf{p}) - 2\rho_{fi}(\mathbf{p}) + g_{fi}(\mathbf{Q},\mathbf{p})}{\mathbf{v}_p \cdot \mathbf{p} - \bar{\varepsilon} + i0}, \quad (11)$$

where

$$g_{fi}(\mathbf{Q},\mathbf{p}) = \langle \Psi_f | e^{i(\mathbf{Q}-\mathbf{p})\cdot\mathbf{r}_1} e^{i\mathbf{p}\cdot\mathbf{r}_2} + e^{i(\mathbf{Q}-\mathbf{p})\cdot\mathbf{r}_2} e^{i\mathbf{p}\cdot\mathbf{r}_1} + 4 | \Psi_i \rangle.$$

### C. Distorted-wave Born approximation

The projectile-target nucleus interaction plays no role in FBA, which assumes single collision between the projectile and the ejected electron and treats the initial and final projectile's states by plane waves. It can be taken into account within the distorted-wave Born approximation (DWBA) [3],

$$\mathcal{T}_{fi}^{\text{DWBA}} = -\langle \psi_{\mathbf{k}_p}^{(-)} \Psi_f | \frac{Z_p}{|\mathbf{r}_1 - \mathbf{R}|} + \frac{Z_p}{|\mathbf{r}_2 - \mathbf{R}|} | \psi_{\mathbf{k}_p}^{(+)} \Psi_i \rangle, \quad (12)$$

where  $\mathbf{R}$  is the C<sup>6+</sup> position,  $\psi_{\mathbf{k}_p}^{(+)}$  and  $\psi_{\mathbf{k}_p}^{(-)}$  are, respectively, the incoming and outgoing distorted waves for C<sup>6+</sup> in the Coulomb field of the target nucleus.

In construction of the distorted waves we involve the straight line or eikonal approximation that proved to be very useful in treatments of near-forward scattering of particles having short de Broglie wavelength. Neglecting the change in the projectile velocity, that is,  $\mathbf{v}_p = \mathbf{v}'_p$ , and assuming the  $z$  axis to be directed along the incident projectile momentum, we get

$$\psi_{\mathbf{k}_p}^{(+)}(\mathbf{R}) = \exp\left(i\mathbf{k}_p \cdot \mathbf{R} - \frac{i}{v_p} \int_{-\infty}^z dz' \frac{Z_p Z_T}{\sqrt{b^2 + z'^2}}\right), \quad (13)$$

$$\psi_{\mathbf{k}_p}^{(-)}(\mathbf{R}) = \exp\left(i\mathbf{k}'_p \cdot \mathbf{R} + \frac{i}{v_p} \int_z^{\infty} dz' \frac{Z_p Z_T}{\sqrt{b^2 + z'^2}}\right), \quad (14)$$

where  $\mathbf{R} = (\mathbf{b}, z)$ , with  $\mathbf{b}$  can be viewed as an impact parameter vector, and  $Z_T$  is the charge of the target nucleus. Substitution of (13) and (14) in (12) yields

$$\mathcal{T}_{fi}^{\text{DWBA}} = \int d^2b (v_p b)^{2i\eta} \int \frac{d^2q}{(2\pi)^2} e^{i\mathbf{q}\cdot\mathbf{b}} \mathcal{T}_{fi}^{\text{FBA}}(\mathbf{Q}-\mathbf{q}), \quad (15)$$

where  $\eta = Z_p Z_T/v_p$  is the Sommerfeld parameter, and  $\mathbf{q}$  is perpendicular to the  $z$  axis. In Eq. (15) we omitted the phase factor  $\lim_{z \rightarrow \infty} (v_p z)^{-2i\eta}$ , which, though being divergent, does not affect the FDCS. Note that the  $\mathbf{b}$  integration in Eq. (15) can be carried out analytically (see the Appendix).

## III. RESULTS AND DISCUSSION

In this section we present numerical results for FDCS in comparison with experimental values [6]. We inspect its dependence on the angle of the ejected electron in two different planes. One is the scattering plane, which is formed by the incident momentum  $\mathbf{k}_p$  and the momentum transfer  $\mathbf{Q}$ . It defines the  $x$ - $z$  plane, with the  $z$  axis chosen to be directed along the incident projectile velocity and the  $x$  axis being directed such that  $Q_x > 0$ . Thus,  $\mathbf{Q} = (Q_x, 0, Q_z)$ , where in the discussed kinematics ( $Q = 0.75$  a.u. and  $E_e = 6.5$  eV),

$$Q_x \simeq 0.75 \text{ a.u.}, \quad Q_z \simeq \frac{T}{v_p} \simeq 0.02 \text{ a.u.}$$

The other defines the  $y$ - $z$  plane and will be referred to as the perpendicular plane because it is practically perpendicular to  $\mathbf{Q}$ . In both planes specified above, the electron angle is measured with respect to the  $z$  axis and is varied from  $0^\circ$  to  $360^\circ$  such that an angle of  $90^\circ$  corresponds to the electron ejection in the positive  $x$  ( $y$ ) direction in the scattering (perpendicular) plane.

In numerical implementation of the theoretical approaches formulated in the previous section, we employ the following models for the initial and final helium states:

$$\Psi_i(\mathbf{r}_1, \mathbf{r}_2) = \phi_{1s}(\mathbf{r}_1; Z_i) \phi_{1s}(\mathbf{r}_2; Z_i), \quad (16)$$

$$\Psi_f(\mathbf{r}_1, \mathbf{r}_2) = \frac{1}{\sqrt{2}} [\phi_{\mathbf{k}_e}^{(-)}(\mathbf{r}_1; Z_e) \phi_{1s}(\mathbf{r}_2; Z_f) + \phi_{\mathbf{k}_e}^{(-)}(\mathbf{r}_2; Z_e) \phi_{1s}(\mathbf{r}_1; Z_f)], \quad (17)$$

where  $\phi_{1s}$  is a hydrogenlike  $1s$  orbital and  $\phi_{\mathbf{k}_e}^{(-)}$  is an outgoing Coulomb wave for the ejected electron. The values of  $Z_i$  and  $Z_f$  are  $Z_i = 27/16$  and  $Z_f = 2$ , while the  $Z_e$  value can be varied in the range  $1 \leq Z_e \leq 2$ . Clearly, the ejected electron experiences the effective charge  $Z_e = 1$  ( $Z_e = 2$ ) far from (close to) the target nucleus.

In spite of their relative simplicity, the functions (16) and (17) efficiently mimic the basic features pertinent to single-ionization processes on helium. For example, they adequately explain the angular distribution of the ejected electron in the scattering plane in the case of the  $(e, 2e)$  experiments at high impact energy and small momentum transfer (see, for instance, the book [22] and references therein). In addition, their use in the calculations makes the numerical implementation more transparent and controllable.

### A. FBA results

The measurements of Schulz *et al.* [6] were performed on a relative intensity scale. In order to put all the calculations and experimental values on a common intensity scale, we normalize the experiment by fitting the measured FDCS value integrated over the ejection angle in the scattering plane to that using FBA (7) in the  $Z_e = 1$  case. The obtained normalization factor is then applied to the experimental data in the perpendicular plane. The results are shown in Fig. 1. Also included in Fig. 1 are the FBA calculations for  $Z_e = 1.5$ , 27/16, and 2 in the final-state helium function, which are scaled by factors of 1.37, 1.69, and 2.64, respectively. Each scaling factor is obtained so that the area under the corresponding curve in the scattering plane is the same as that in the  $Z_e = 1$  case.

As can be seen from Fig. 1, in the scattering plane all the FBA calculations exhibit similar qualitative features as the experimental angular distribution of the ejected electron. Namely, they exhibit the binary peak at around  $90^\circ$ , which corresponds to the electron ejection in the direction of the momentum transfer, and the so-called recoil peak at around

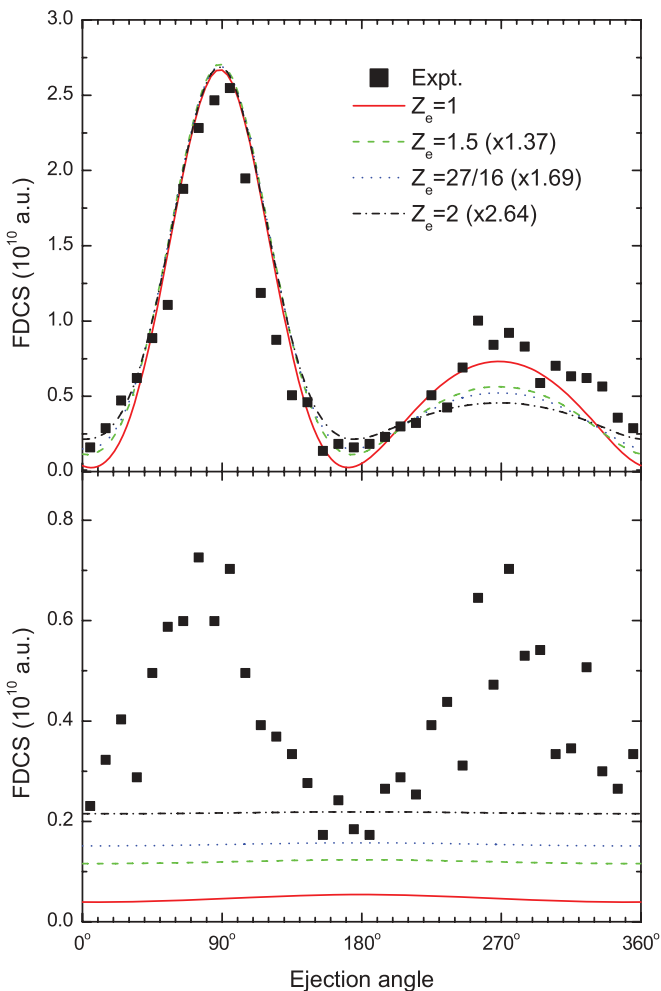


FIG. 1. (Color online) FBA results for the FDCS as a function of the angle of the ejected electron in the scattering (top) and perpendicular (bottom) planes. All the experimental and theoretical FDCS values are shown as normalized intensities relative to the FBA cross section for  $Z_e = 1$ . See text for details.

$270^\circ$ , which corresponds to the electron ejection in the direction of the momentum transfer followed by the electron recoil from the target nucleus in the opposite direction. The best overall agreement with experiment in the scattering plane is found in the  $Z_e = 1$  case. However, marked discrepancies between experiment and the FBA results are determined in the perpendicular plane, both in terms of intensity and in terms of shape. In particular, FBA yields almost a flat angular distribution while the experiment exhibits well-pronounced peaks at ejection angles of  $90^\circ$  and  $270^\circ$ . It is remarkable that similar results are obtained using more accurate models of the initial and final states of helium. This indicates that the observed discrepancies between FBA and experiment are unlikely to be related to the quality of the helium wave functions employed in the calculations (see also Ref. [9]).

### B. Relativistic effects

Relativistic corrections to the nonrelativistic FBA amplitude can be estimated using Eq. (6). Since  $\mathbf{j} = (\rho\mathbf{v} + \mathbf{v}\rho)/2$ , where  $\mathbf{v}$  is the electron velocity operator, the ratio

$$\frac{\mathbf{v}_p \cdot \mathbf{j}_{fi}(\mathbf{Q})}{c^2 \rho_{fi}(\mathbf{Q})}$$

introduces a correction of the order of  $v_p v_a / c^2$ , where  $v_a$  is a characteristic velocity of atomic electrons. Though  $v_p / c$  is almost  $1/2$ , this correction is very minor, because the electrons in helium, both in the initial and in the final state, are nonrelativistic. The factor,

$$\frac{1}{1 - \frac{T^2}{Q^2 c^2}} \sqrt{\frac{E_p}{E'_p}},$$

does not depend on the angle of the ejected electron and its value is very close to unity, which means that it practically does not affect the FDCS. Thus, it is clear that the relativistic effects are not responsible for the discrepancy between FBA and experiment in the perpendicular plane. Note that treating the projectile fully nonrelativistically implies that  $E'_p / c^2 = M_p$  in Eq. (1). In the case of the discussed kinematics, it means scaling down of the FDCS by a factor of about 1.23 (see also Ref. [9]).

### C. Second-order effects

SBA results for FDCS are shown in Fig. 2 together with experimental values and those using FBA for  $Z_e = 1$ . The normalization and scaling procedures are the same as in Fig. 1. The SBA values were obtained in the closure approximation (11). We find very low sensitivity of the calculations to the closure parameter (10). The SBA results shown in Fig. 2 correspond to  $\bar{\epsilon} = 24.59$  eV, which is the first ionization potential of He. It can be seen that SBA is practically indistinguishable from FBA in the scattering plane, and it only slightly differs from FBA in the perpendicular plane. This supports results of other SBA calculations [9,20] with more accurate helium wave functions.

### D. Effects of distortion

Figure 3 compares results of the DWBA calculations based on Eq. (15) with experiment. Also shown in Fig. 3 are FBA

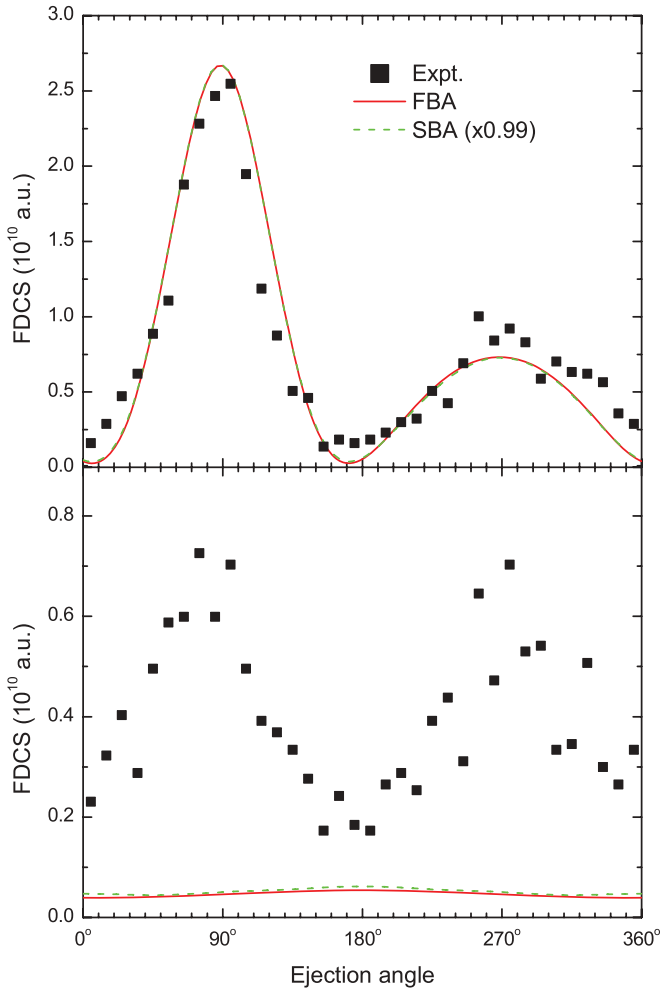


FIG. 2. (Color online) The SBA values for the FDCS in the scattering (top) and perpendicular (bottom) planes. All the experimental and theoretical FDCS values are shown as normalized intensities relative to the FBA cross section for  $Z_e = 1$ . See text for details.

results for  $Z_e = 1$ . The normalization and scaling procedures are the same as in Fig. 1. Three different values of the effective charge of the target nucleus are examined. The value  $Z_T = 2$  corresponds to the case of the unscreened, bare nucleus, while  $Z_T = 1$  to the maximal screening effect due to the electron that remains bound in  $He^+$ . We also consider here the value  $Z_T = 1.34$  that was utilized in similar calculations of Ref. [18], where, however, the so-called time-dependent close-coupling approach (TDCC) was used instead of FBA [see Eq. (15)]. There it was found that theory not only well describes experiment in the scattering plane but also exhibits a two-peak structure similar to the experiment in the perpendicular plane, though still notably underestimating the experimental intensity in that geometry. The present calculations do not confirm the conclusion of Ref. [18]. Moreover, we can see in Fig. 3 that the distortion effects in the perpendicular plane slightly change the FBA angular distribution, leading to a one-peak structure with the maximum at  $180^\circ$ , where, in contrast, one finds a dip in the experimental angular distribution.

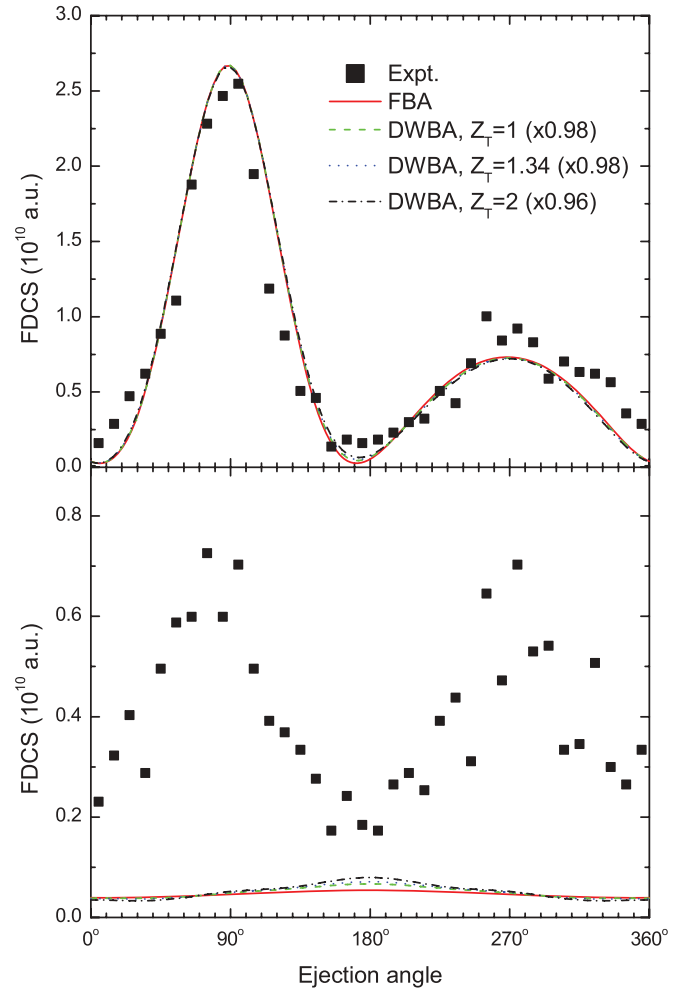


FIG. 3. (Color online) The DWBA values for the FDCS in the scattering (top) and perpendicular (bottom) planes. All the experimental and theoretical FDCS values are shown as normalized intensities relative to the FBA cross section for  $Z_e = 1$ . See text for details.

### E. Effects of experimental uncertainties

In order to make the quantitative comparisons with experiment more accurate, one must take into account experimental uncertainties, which are generally of two types. One type is associated with a finite energy and angular resolution of the detectors, and the other with finite widths of the initial projectile and target wave packets in momentum space. Thus, theoretical values must be broadened by the experimental resolution and by the initial projectile and target momentum distributions (see, for instance, a very useful book of Taylor [3]). In the case of discussed measurements the broadening can be largely due to the velocity spread of the He gas atoms in a supersonic jet. This spread results in the uncertainty of the measured momentum transfer, because in the experiment of Schulz *et al.* [6] its value was determined, through the momentum conservation law, by measuring the momenta of the ejected electron and the recoil  $He^+$  ion. The most frequently used velocity distribution function is an ellipsoidal drifting Maxwellian model which assumes Gaussian distributions with different widths in the longitudinal and transverse directions of

the jet (see, for instance, Ref. [23] and references therein). The widths are determined by the temperature of the He gas atoms. In the present analysis we take the broadening into account by convoluting the FBA cross sections with a two-dimensional Gaussian function,

$$P(Q'_x, Q'_y) = \frac{1}{2\pi\sigma_x\sigma_y} \exp \left[ -\frac{(Q'_x - Q_x)^2}{2\sigma_x^2} - \frac{(Q'_y - Q_y)^2}{2\sigma_y^2} \right],$$

$$\sigma_{x(y)} = \frac{\Delta Q_{x(y)}}{2\sqrt{2 \ln 2}}, \quad (18)$$

where  $Q_x \simeq 0.75$  a.u.,  $Q_y = 0$  a.u., and  $\Delta Q$  is the full width at half maximum (FWHM). The convoluted FDCS is thus given by

$$\frac{d^3\sigma}{dE_e d\Omega_e d\Omega_p} = \int_{-\infty}^{\infty} dQ'_x \int_{-\infty}^{\infty} dQ'_y P(Q'_x, Q'_y) \times \frac{k_e E_p'^2 k'_p}{(2\pi)^5 c^4 k_p} |\mathcal{T}_{fi}^{\text{FBA}}|^2, \quad (19)$$

where  $\mathbf{k}'_p = \mathbf{k}_p - \mathbf{Q}'$ ,  $E_p' = c^2 \sqrt{k_p'^2 + M_p^2 c^2}$ , and  $\mathcal{T}_{fi}^{\text{FBA}}$  is evaluated in accordance with Eq. (7) at the momentum transfer  $\mathbf{Q}' = (Q'_x, Q'_y, Q_z)$ . Note that the uncertainty of the  $z$  component of the momentum transfer is negligible, because it is given by  $\Delta Q_z \simeq \Delta T/v_p$ , where  $v_p \simeq 59$  a.u. and the uncertainty of the energy transfer is  $\Delta T \ll 1$  a.u. [14].

The results of the convolution of the FBA calculations in the  $Z_e = 1$  case with the momentum distribution function (18) are presented in Fig. 4 in comparison with experiment. The normalization and scaling procedures are the same as in Fig. 1. Different values of the momentum uncertainties,  $\Delta Q_x$  and  $\Delta Q_y$  (or FWHM), are considered. The case of no uncertainties, that is,  $\Delta Q_x = \Delta Q_y = 0$ , amounts to unconvoluted FBA calculations, while the FWHM values  $\Delta Q_x = 0.23$  a.u. and  $\Delta Q_y = 0.46$  a.u. were reported in Ref. [15] and they are supposed to correspond to the temperature of the He gas atoms of 1–2 K [14,15]. It can be seen that the inclusion of the uncertainties according to Ref. [15] insignificantly influences the FBA calculations in the scattering plane and only slightly reduces the large discrepancy in intensity between theory and experiment in the perpendicular plane. At the same time, it changes the theoretical angular distribution in the perpendicular plane so that it resembles the experimental two-peak structure. The latter observation hints at the importance of the experimental uncertainties' effects in the perpendicular plane. This is illustrated in Fig. 4 by the results of convolution of the FBA calculations with the momentum uncertainties  $\Delta Q_x = 0.65$  a.u. and  $\Delta Q_y = 1.3$  a.u. These values correspond to the temperature of the He gas atoms of 8–16 K, which is eight times larger than that of Ref. [15]. Remarkably, increasing the temperature provides reasonable agreement between theory and experiment in the perpendicular plane, though it somewhat worsens the agreement in the scattering plane. This finding supports the results of Ref. [13], where the continuum distorted wave calculations were convoluted with experimental uncertainties. However, in contrast to the present study, the authors of Ref. [13] did not explicitly specify the FWHM values they used in their computations.

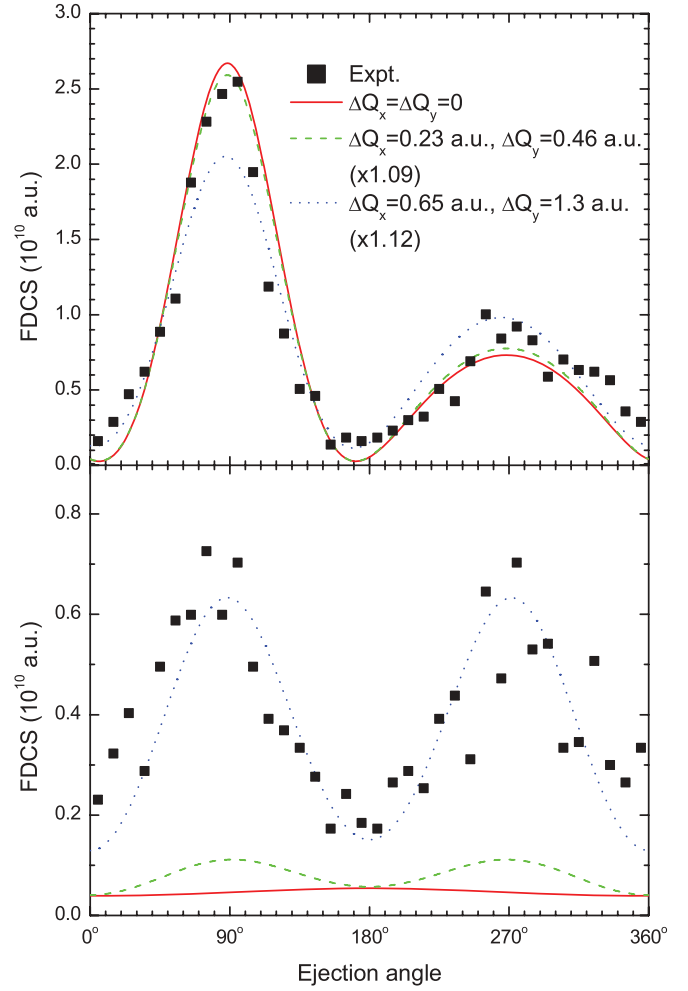


FIG. 4. (Color online) The FBA values for the FDCS in the scattering (top) and perpendicular (bottom) planes convoluted with experimental uncertainties. All the experimental and theoretical FDCS values are shown as normalized intensities relative to the FBA cross section for  $Z_e = 1$ . See text for details.

#### IV. SUMMARY AND CONCLUSIONS

In summary, we have carried out a theoretical investigation of the  $C^{6+}$  problem using simple models of the initial and final helium states. Different well-established approximations have been involved. Numerical calculations of FDCS using these approximations have been performed and their results have been compared to the experimental values in the scattering and perpendicular planes. Reasonable agreement with experiment has been found in the scattering plane, which is in accord with other theoretical studies. The numerical results for FDCS in the perpendicular plane are in drastic disagreement with experiment, thus supporting the findings of previous theoretical investigations. Various effects beyond the nonrelativistic FBA for the scattering amplitude have been inspected. It has been deduced that the relativistic effects practically do not change the FBA amplitude. At the same time, it has been emphasized that the relativistic treatment of kinematical variables of the projectile seriously influences the absolute FDCS value, scaling it up by a factor of 1.23 compared to the case of the nonrelativistic treatment. The second-order

and distorted-wave effects have been shown to have a minor impact on the electron angular distribution. We have found that the experimental uncertainties can dramatically influence the electron emission pattern in the perpendicular plane. It has been demonstrated that at certain temperatures of the He gas atoms in a supersonic jet these uncertainties can explain much of the observed differences between theory and experiment.

Some comments should be made regarding the absolute normalization of the experimental data. It can be noted that the normalization procedure utilized in our study differs from that of Ref. [7], where the total number of recoiling He<sup>+</sup> ions with momenta smaller than 10 a.u. measured in coincidence with the ionized electron energy from 0 to 50 eV were normalized to the corresponding part of the total single ionization cross section given by the FBA approach with Hartree-Fock wave functions for the active electron (FBA-HF). Such normalization might be more accurate than the present one, but it would demand a huge computational effort in order to obtain the scaling factors for all the theories examined in this work. In addition, the choice of the normalization procedure does not influence the electron emission patterns, which have been the main focus of our analysis.

The results of the discussed experiment challenge our well-established theoretical methods developed for the treatment of the atomic ionization processes induced by impact of fast charged massive particles. It can be concluded that at present no theory is able to explain the observed serious disagreement with experiment. Unfortunately, the recent promising results of Colgan *et al.* [18], which exhibited at least qualitative agreement with experiment by taking into account the phase shift due to the internuclear interaction, are not supported by the present analysis as well as by another very recent study [20]. Following conclusions made in Ref. [6], this situation seems to suggest that we should revise our basic theoretical understanding and develop new theoretical concepts for the few-body atomic processes. In this connection, some comments should be made regarding the conjecture recently made by Egodapitiya *et al.* [24] that the proper account for the localization of the C<sup>6+</sup> projectile in the experiment [6] could probably solve the longstanding problem. There are two important differences between measurements of Refs. [6] and [24]. First, the localization of the projectile wave packet in the singly ionizing 75-keV  $p + \text{H}_2$  collisions studied in Ref. [24] can be crucial for observing an interference pattern from the two scattering centers, while in the C<sup>6+</sup>+He case [6] one deals with a one-center scattering problem where that kind of interference is always absent. Second, Egodapitiya *et al.* [24] measured the energy and angle of the scattered projectile, while Schulz *et al.* [6] determined those values indirectly as mentioned earlier. Implications of the latter fact are better demonstrated within FBA, where the scattering amplitude depends only on  $\mathbf{Q}$ . Indeed, after convoluting the FBA cross section with the initial projectile wave packet in momentum space (see, for instance, Ref. [3]), we find that in measurements of Schulz *et al.* [6] the effect of the projectile localization cancels, while in those of Egodapitiya *et al.* [24] it does not, because here it affects the  $\mathbf{Q}$  value. What becomes important in the case of Ref. [6], in contrast to the case of Ref. [24], is the localization of the target wave packet in momentum space. In our analysis we effectively took into account this localization

(or the velocity spread of the He atoms) by convoluting the FBA cross section with the momentum distribution function (18).

Thus, an important question arises: Is the discussed discrepancy due to theory or can it be attributed to experiment? Let us recall that one of the cornerstones of physics is reproducibility of measurements. Taking into account that already a lot of theoretical efforts have been devoted to the problem, the new, independent measurements are highly desirable to shed more light on the ‘‘C<sup>6+</sup> puzzle’’.

#### ACKNOWLEDGMENTS

We thank M. Schulz for valuable comments and H. R. J. Walters for useful discussions. The research of two of the authors (K.A.K. and Yu. V. P.) is supported by the Russian Foundation for Basic Research (Grant No. 11-01-00523-a).

#### APPENDIX: INTEGRAL OVER THE IMPACT PARAMETER VECTOR

Consider two-dimensional integration over  $\mathbf{b}$  in Eq. (15). Since  $\mathcal{T}_{fi}^{\text{FBA}}$  in the integrand does not depend on the impact parameter vector, the  $\mathbf{b}$  integration reduces to

$$I(q; v_p, \eta) = \int_0^\infty db b (v_p b)^{2i\eta} \int_0^{2\pi} d\varphi e^{iqb \cos \varphi}. \quad (\text{A1})$$

Integration over  $\varphi$  gives

$$I(q; v_p, \eta) = 2\pi \int_0^\infty db b (v_p b)^{2i\eta} J_0(qb), \quad (\text{A2})$$

where  $J_0$  is the Bessel function of zeroth order. Using the tabulated integrals [25] for combinations of Bessel functions, exponentials, and powers, we get

$$\begin{aligned} I(q; v_p, \eta) &= 2\pi \lim_{\lambda \rightarrow 0} \int_0^\infty db e^{-\lambda b} b (v_p b)^{2i\eta} J_0(qb) \\ &= 2\pi v_p^{2i\eta} \lim_{\lambda \rightarrow 0} \frac{\Gamma(2 + 2i\eta)}{(\lambda^2 + q^2)^{1+i\eta}} \\ &\quad \times {}_2F_1\left(1 + i\eta, -\frac{1}{2} - i\eta; 1; \frac{q^2}{\lambda^2 + q^2}\right), \end{aligned} \quad (\text{A3})$$

where  ${}_2F_1$  is a hypergeometric function. Since [25]

$${}_2F_1\left(1 + i\eta, -\frac{1}{2} - i\eta; 1; 1\right) = \frac{\Gamma(\frac{1}{2})}{\Gamma(-i\eta)\Gamma(\frac{3}{2} + i\eta)}, \quad (\text{A4})$$

we find

$$I(q; v_p, \eta) = \frac{2\pi}{q^2} \left(\frac{v_p}{q}\right)^{2i\eta} \frac{\Gamma(\frac{1}{2})\Gamma(2 + 2i\eta)}{\Gamma(-i\eta)\Gamma(\frac{3}{2} + i\eta)}. \quad (\text{A5})$$

Using (A5) in (15), we obtain

$$\begin{aligned} \mathcal{T}_{fi}^{\text{DWBA}} &= \frac{\Gamma(\frac{1}{2})\Gamma(2 + 2i\eta)}{\Gamma(-i\eta)\Gamma(\frac{3}{2} + i\eta)} \lim_{\epsilon \rightarrow 0} \int_0^\infty \frac{dq}{q^{1-\epsilon}} \left(\frac{v_p}{q}\right)^{2i\eta} \\ &\quad \times \int_0^{2\pi} \frac{d\varphi_q}{2\pi} \mathcal{T}_{fi}^{\text{FBA}}(\mathbf{Q} - \mathbf{q}), \end{aligned} \quad (\text{A6})$$

where an infinitesimal  $\epsilon$  is introduced for regularization of the integral over  $q$ .

- [1] L. D. Landau and E. M. Lifshitz, *Quantum Mechanics: Nonrelativistic Theory*, 3rd ed. (Pergamon, Oxford, 1977).
- [2] V. B. Berestetskii, E. M. Lifshitz, and L. P. Pitaevskii, *Quantum Electrodynamics*, 2nd ed. (Butterworth-Heinemann, Oxford, 1982).
- [3] J. R. Taylor, *Scattering Theory: The Quantum Theory of Nonrelativistic Collisions* (Wiley, New York, 1972).
- [4] J. Ullrich, R. Moshhammer, R. Dörner, O. Jagutzki, V. Mergel, H. Schmidt-Böcking, and L. Spielberger, *J. Phys. B* **30**, 2917 (1997).
- [5] J. Ullrich, R. Moshhammer, A. Dorn, R. Dörner, L. Ph. H. Schmidt, and H. Schmidt-Böcking, *Rep. Prog. Phys.* **66**, 1463 (2003).
- [6] M. Schulz, R. Moshhammer, D. Fischer, H. Kollmus, D. H. Madison, S. Jones, and J. Ullrich, *Nature (London)* **422**, 48 (2003).
- [7] D. Madison, M. Schulz, S. Jones, M. Foster, R. Moshhammer, and J. Ullrich, *J. Phys. B* **35**, 3297 (2002).
- [8] A. B. Voitkiv, B. Najjari, and J. Ullrich, *J. Phys. B* **36**, 2591 (2003).
- [9] M. McGovern, C. T. Whelan, and H. R. J. Walters, *Phys. Rev. A* **82**, 032702 (2010).
- [10] M. F. Ciappina and W. R. Cravero, *J. Phys. B* **39**, 1091 (2006).
- [11] A. L. Harris, D. H. Madison, J. L. Peacher, M. Foster, K. Bartschat, and H. P. Saha, *Phys. Rev. A* **75**, 032718 (2007).
- [12] M. McGovern, D. Assafrão, J. R. Mohallem, C. T. Whelan, and H. R. J. Walters, *Phys. Rev. A* **81**, 042704 (2010).
- [13] J. Fiol, S. Otranto, and R. E. Olson, *J. Phys. B* **39**, L285 (2006).
- [14] M. Durr, B. Najjari, M. Schulz, A. Dorn, R. Moshhammer, A. B. Voitkiv, and J. Ullrich, *Phys. Rev. A* **75**, 062708 (2007).
- [15] M. Schulz, M. Dürr, B. Najjari, R. Moshhammer, and J. Ullrich, *Phys. Rev. A* **76**, 032712 (2007).
- [16] M. Schulz, *Phys. Scr.* **80**, 068101 (2009).
- [17] M. F. Ciappina, T. Kirchner, and M. Schulz, *Comput. Phys. Commun.* **181**, 813 (2010).
- [18] J. Colgan, M. S. Pindzola, F. Robicheaux, and M. F. Ciappina, *J. Phys. B* **44**, 175205 (2011).
- [19] M. S. Pindzola, F. Robicheaux, and J. Colgan, *Phys. Rev. A* **82**, 042719 (2010).
- [20] H. R. J. Walters and C. T. Whelan, *Phys. Rev. A* **85**, 062701 (2012).
- [21] V. L. Shablov, P. S. Vinitzky, Yu. V. Popov, O. Chuluunbaatar, and K. A. Kouzakov, *Phys. Part. Nucl.* **41**, 335 (2010).
- [22] R. K. Peterkop, *Theory of Ionization of Atoms by Electron Impact* (Colorado Associated University Press, Boulder, 1977).
- [23] D. R. Miller, in *Atomic and Molecular Beam Methods*, edited by G. Scoles, Vol. 1 (Oxford University Press, Oxford, 1988), p. 14.
- [24] K. N. Egodapitiya, S. Sharma, A. Hasan, A. C. Laforge, D. H. Madison, R. Moshhammer, and M. Schulz, *Phys. Rev. Lett.* **106**, 153202 (2011).
- [25] I. S. Gradshteyn and I. M. Ryzhik, *Table of Integrals, Series, and Products*, 7th ed. (Academic Press, Oxford, 2007).